Available online at www.sciencedirect.com
ScienceDirect
Journal of the European Ceramic Society 30 (2010) 583–589
www.elsevier.com/locate/jeurceramsoc

Two-Step Sintering of oxide ceramics with various crystal structures

Karel Maca *, Vaclav Pouchly, Pavel Zalud

Department of Ceramics and Polymers, Brno University of Technology, Brno, Czech Republic

Available online 4 July 2009

Abstract

The influence of Two-Step Sintering (TSS) process on the final microstructure of oxide ceramic materials with three different crystal structures was studied. Two kinds of alumina (particle size 100 nm resp. 240 nm) as well as tetragonal zirconia (stabilized with 3 mol% Y_2O_3, particle size 60 nm) and cubic zirconia (8 mol% Y_2O_3, 140 nm) powders were cold isostatically pressed and pressurelessly sintered with different heating schedules. The microstructures achieved with TSS method were compared with microstructures achieved with conventional Single-Step Sintering (SSS) schedule. The results showed that the efficiency of the TSS of these oxide ceramics was more dependent on their crystal structure than on their particle size and green body microstructure. The method of TSS brought only negligible improvement of the microstructure of tetragonal zirconia and hexagonal alumina ceramics. On the other hand, TSS was successful in the sintering of cubic zirconia ceramics; it led to a decrease in grain size by a factor of 2.

Keywords: Two-Step Sintering; Grain size; Microstructure-final; Al_2O_3; ZrO_2

1. Introduction

The goal of the sintering process of advanced ceramic materials is most frequently to obtain a material with a high relative density and homogeneous microstructure consisting of small grains. It is well known that the sintering behavior and final grain size are influenced, in particular, by the size of the particles of input ceramic material, degree of its agglomeration, and also by the microstructure of green body, which in addition to the properties of powder material is also determined by the shaping technology used.[1–4] No unified opinion can as yet be found in the literature as to whether the final grain size of an individual body of a defined final density can also be influenced by the choice of sintering regimes. There are papers showing that final density definitely determines the grain size of the sintered bodies.[5–10] On the other hand, there are also reports which claim that choosing correctly the sintering cycle enables obtaining a refined microstructure of materials. Based on such concepts are, for example, the Rapid-Rate Sintering,[11,12] Rate-Controlled Sintering,[13–15] and Two-Step Sintering.[16–32]

The Two-Step Sintering (TSS in the following) procedure consists of the following steps: (1) sintering at a constant heating rate until the relative sample density >75% t.d. is achieved; (2) temperature decrease by ca. 100 °C and sample sintering for a period of tens of hours at a lowered temperature. The authors of the method[16] claim that the first step guarantees the disappearance of supercritical pores while the other pores become unstable so that the body can subsequently sinter at a lower temperature. At the same time, the growth of grains is limited at the lower temperature of the second sintering step and the TSS thus yields a body of identically high density but with smaller grains than could be obtained using the usual constant heating rate cycle with a dwell time at the sintering temperature (so called Single-Step Sintering, SSS in the following).

So far, the TSS method has been used with great success in ceramic materials of cubic structure such as Y_2O_3,[16,17] $BaTiO_3$,[18–20] $SrTiO_3$,[21,22] c-ZrO_2,[23,24] and $CoFe_2O_4$,[25] but with less successful examples in tetragonal zirconia[22,26–28] and hexagonal alumina ceramics.[29–32] Achieving a high density and, at the same time, a small grain size is very important for the latter two kinds of structural ceramic materials because it can bring about an improvement of mechanical properties such as hardness,[33] wear resistance,[34] strength[35] or fracture toughness[36] or in the case of alumina also optical transparency.[37]

In this work we present the results of the TSS of two types of alumina and two types of zirconia ceramics. It was examined whether, with the same final density achieved, TSS led to a smaller final grain size than the conventional SSS. While the alumina powders differed only in particle size, the zirconia powders differed in particle size as well as in yttria content (3 or 8 mol%

* Corresponding author. Tel.: +420 541143344; fax: +420 541143202.
E-mail address: maca@fme.vutbr.cz (K. Maca).

0955-2219/$ – see front matter © 2009 Elsevier Ltd. All rights reserved.
doi:10.1016/j.jeurceramsoc.2009.06.008

Table 1
BET particle size of ceramic powders used.

Powder	Producer	Grade	Abbreviation	D_{BET} [nm]
Al_2O_3	Taimei Chemicals, Japan	Taimicron TM-DAR	TAI	100
Al_2O_3	Malakoff Industries, USA	RC-HP DBM	REY	240
ZrO_2 (+3 mol% Y_2O_3)	Tosoh Corporation, Japan	TZ-3YB	Z3Y	60[a]
ZrO_2 (+8 mol% Y_2O_3)	Tosoh Corporation, Japan	TZ-8YSB	Z8Y	140[a]

[a] Values of specific surface area given by the producer.

of Y_2O_3) and therefore in crystal structure (tetragonal or cubic). The aim of this paper was to assess the effect of particle size and crystal structure on the efficiency of the TSS method.

2. Experimental

2.1. Materials

Four types of commercially available ceramic powders were used. The details of these powders are given in Table 1. The particle size D_{BET} was calculated from the specific surface area established by nitrogen absorption (BET method, ChemBet 3000, Quantachrome, USA). The following values of theoretical densities were used for the calculation of average particle size from the specific surface area (as well as in the calculation of relative densities below): $\rho_{th}(TAI) = \rho_{th}(REY) = 3.99\ g\ cm^{-3}$; $\rho_{th}(Z3Y) = 6.08\ g\ cm^{-3}$; $\rho_{th}(Z8Y) = 5.99\ g\ cm^{-3}$.

2.2. Preparation of ceramic green bodies

Disks of 30 mm in diameter and ca. 5 mm in height were prepared from the above materials, via cold isostatic pressing (CIP). Pressing was carried out in an isostatic press (Autoclave Engineering, Inc., USA) at a pressure of 300 MPa with a dwell time of 5 min. The CIPed samples were pre-sintered at 800 °C/1 h, then cut and ground to the shape of prisms of ca. 4 mm × 4 mm × 15 mm for sintering in a dilatometer, or 8 mm × 8 mm × 10 mm for sintering in a conventional furnace. The pore size distribution in green bodies was measured by mercury intrusion porosimetry (Pascal 440, Porotec, Germany).

2.3. Sintering of ceramic bodies

The samples were first sintered in a high-temperature dilatometer (L70/1700, Linseis, Germany) with a view to easily finding the temperature of the first sintering step (T_1). The relative density of the sintered sample should be between 75% t.d. and 92% t.d.,[17] the sintering shrinkage curves were therefore recalculated to the densification profiles. The details of such recalculation are described elsewhere.[38]

TSS and SSS experiments were performed in a superkanthal resistance furnace (K1700/1, Heraeus, Germany) in air atmosphere. In the case of TSS several combinations of temperatures of the first sintering step (T_1) and the second sintering step (T_2) were tested for each material. Sintering proceeded at a heating rate of 10 °C/min up to a temperature of 800 °C, and at 5 °C/min up to a temperature of the first sintering step (i.e. the same heating rates as in the previous dilatometric sintering experiments). The temperature decreases from the first to the second sintering step proceeded at a rate of 60 °C/min. The dwell times at the T_2 temperature were 0, 5, 10, 15, and 20 h.

To enable a comparison of the TSS method with the conventional SSS, some bodies were also sintered in a mode with constant temperature increase and a dwell time at the sintering temperature.

2.4. Study of microstructure of sintered samples

The final relative densities of samples (ρ_{rel}) were determined on the basis of Archimedes' principle (EN 623-2) with distilled water and using the above-mentioned theoretical densities. The samples were ground and polished by standard ceramographic methods and then thermally etched (at T_2 for 7 min) to expose the grain boundaries. The microstructure of samples was studied using scanning electron microscopy (Philips XL30, the Netherlands). The grain size (D) was estimated by the linear intercept method (EN 623-3). For each sample, at least three photographs were taken of the microstructure; in each microphotograph a minimum of five line segments were assessed.

3. Results and discussion

3.1. Selection of temperatures of first and second sintering steps

The temperatures of the first sintering step for Al_2O_3 and ZrO_2 were chosen on the basis of the evaluation of dilatometric measurements (see Fig. 1). Drawing on data from the literature,[17] temperatures guaranteeing relative densities between 75% t.d. and 92% t.d. were chosen for the first sintering step. The temperatures at which all four materials reached the densities of 75% t.d. and 92% t.d. are given in Table 2.

The temperature of the second sintering step (T_2) was lower than T_1; the decrease from T_1 to T_2 was tested in the range of 30–150 °C.

Table 2
Temperatures at which ceramic materials reach relative density of 75% t.d. or 92% t.d.

Powder	Abbreviation	ρ_{rel} = 75% t.d., T [°C]	ρ_{rel} = 92% t.d., T [°C]
Al_2O_3	TAI	1255	1337
Al_2O_3	REY	1338	1476
ZrO_2 (+3 mol% Y_2O_3)	Z3Y	1263	1343
ZrO_2 (+8 mol% Y_2O_3)	Z8Y	1381	1462

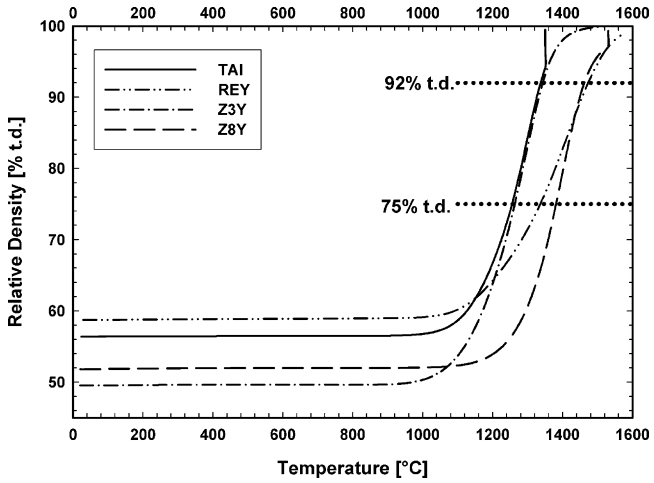

Fig. 1. Densification curves of the ceramic materials used.

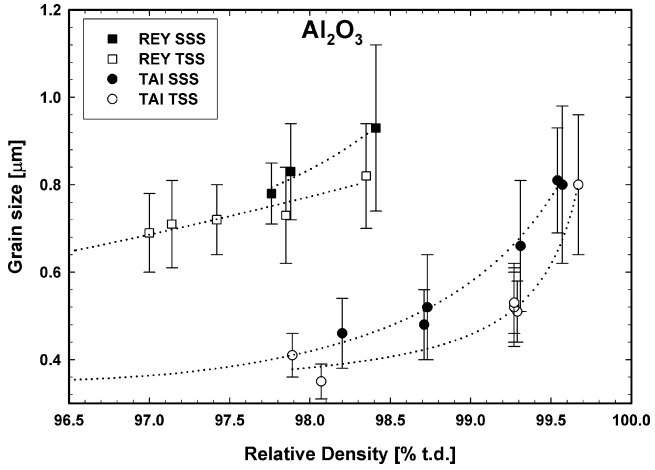

Fig. 3. Dependence of grain size on sintered density of alumina samples sintered by TSS and SSS methods.

3.2. The influence of particle size on the efficiency of Two-Step Sintering of alumina ceramics

Two different alumina powders with different particle sizes (see Table 1) were used in this work. Although the same shaping technology was applied to both samples, the sintering behavior was quite different (see Fig. 1). Despite its higher green density, the sintering kinetics of the REY sample was much slower than that of the TAI sample—for a full densification of the REY sample a temperature higher than 1500 °C was necessary while the TAI sample fully sintered at a temperature of 1350 °C.

As mentioned in Section 1, the sintering behavior of the ceramic body is strongly influenced by the microstructure of the green body.[1–4] Fig. 2 shows the pore size distribution of both alumina samples. It can be seen that pores in the TAI sample were more than twice smaller than in the REY sample. This can be the cause of the worse sintering behavior of the REY sample.

It follows from the previous results that we prepared two different alumina samples with different particle sizes, different pore sizes and different sintering behavior. With these different alumina ceramics we tested the efficiency of the TSS method, i.e. the chance to decrease the grain size of sintered samples. The results of TSS experiments are compared with the results of SSS experiments in Fig. 3.

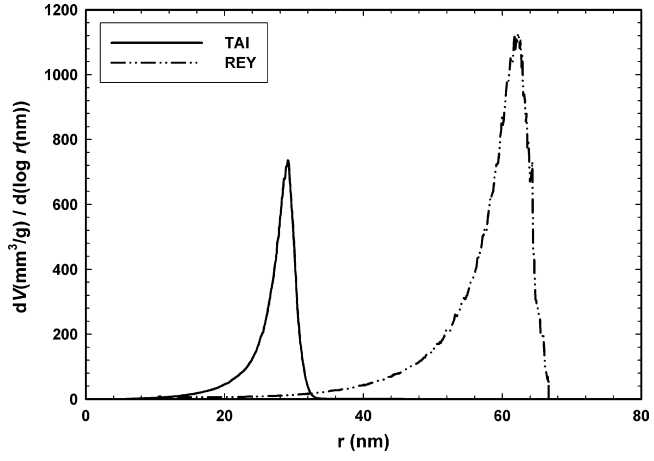

Fig. 2. Pore size distributions of green bodies of alumina (TAI and REY) ceramics.

It can be seen that for both types of alumina the grains were smaller after TSS, but this decrease was only within the standard deviation of grain size evaluation.

The microstructures of the alumina samples sintered to the same final densities by TSS and SSS cycles are given in Fig. 4 (TAI) and Fig. 5 (REY). There are no significant differences between the grain sizes obtained by TSS and SSS. A more precise evaluation of the grain size can be obtained by the linear intercept method. Selected values of final relative densities and grain sizes are given in Table 3. The decrease in the grain size with TSS was ca. 22% for the TAI sample and 12% for the REY sample. Similar results were recently published for Taimicron alumina shaped by uniaxial pressing[31,32] or uniaxial pressing followed by cold isostatic pressing.[31] The low efficiency of the TSS method is explained as a consequence of the small difference between the activation energy of sintering and the grain growth in the case of alumina ceramics.

3.3. The influence of particle size and crystal structure on the efficiency of Two-Step Sintering of zirconia ceramics

Two types of zirconia powder (both prepared by the same manufacturing process by the same producer) were used in this work. Tetragonal zirconia powder (Z3Y) was doped with 3 mol% Y_2O_3 and had a particle size of 60 nm, cubic zirconia powder (Z8Y) was doped with 8 mol% Y_2O_3 and had a particle size of 140 nm.

The pore size distributions of zirconia green bodies (see Fig. 6) were similar to those of alumina green bodies—the sample prepared from the coarser powder had larger pores. Moreover, there were more similarities between the alumina and zirconia samples—the particle size ratio of coarser and finer powder as well as the pore size ratio of samples made from these powders were close to the value 2.4, and this was valid for both alumina and zirconia.

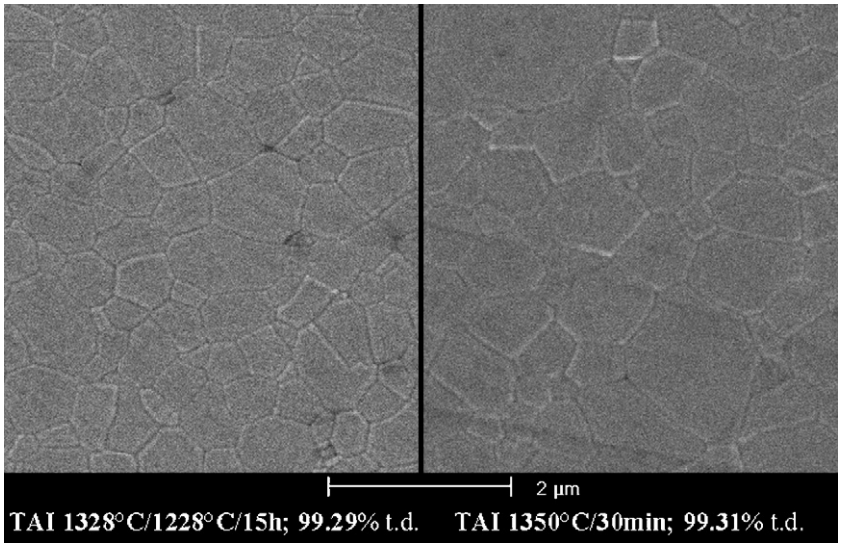

Fig. 4. Microstructure of TAI samples sintered to the same density 99.3% t.d. by TSS and SSS cycles.

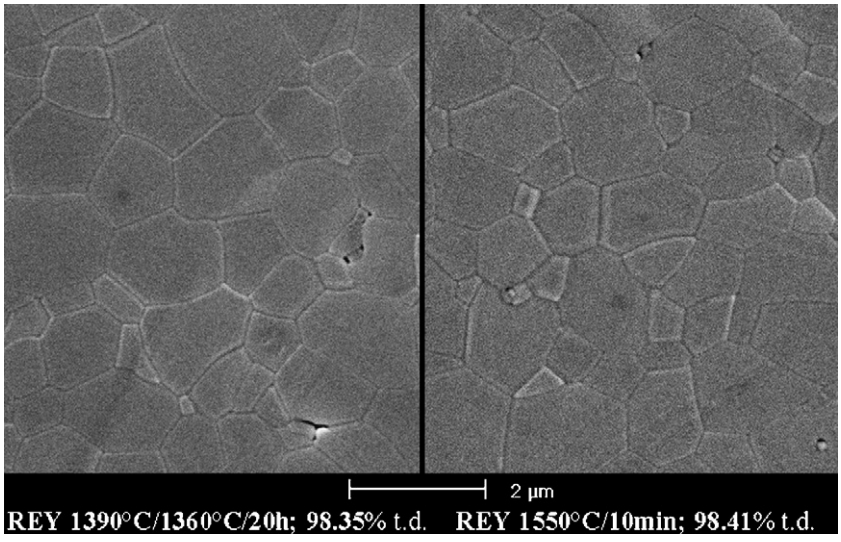

Fig. 5. Microstructure of REY samples sintered to the same density 98.4% t.d. by TSS and SSS cycles.

While in the case of alumina ceramics the efficiency of TSS was only negligible for both finer and coarser powder, we found a big influence of the TSS method on microstructure refinement of cubic zirconia ceramics (see Fig. 7). While in the case of Z3Y sample the grain size was the same for both TSS and SSS up to a final density of 99.6% t.d., the grain size of Z8Y sample sintered by TSS was two times lower than the grain size of the sample sintered by SSS, and this was valid in the interval of final

Table 3
Comparison of densities and grain sizes of samples prepared by conventional SSS and TSS cycles.

Material	Single-Step Sintering				Two-Step Sintering			
	Sintering [°C/min]	ρ_{rel} [% t.d.]	D [μm]	s/n [μm/–]	Sintering [°C/°C/h]	ρ_{rel} [% t.d.]	D [μm]	s/n [μm/–]
TAI	1350/30	99.31	0.66	0.15/30	1328/1228/15	99.29	0.51	0.07/20
REY	1550/1	97.88	0.83	0.11/15	1390/1360/15	97.85	0.73	0.11/15
REY	1550/10	98.41	0.93	0.19/15	1390/1360/20	98.35	0.82	0.12/15
Z3Y	1405/0	98.76	0.16	0.018/15	1305/1275/10	98.73	0.17	0.017/25
Z3Y	1450/0	99.62	0.15	0.023/20	1330/1275/15	99.60	0.18	0.019/25
Z8Y	1530/60	99.32	3.01	0.560/30	1440/1290/15	99.31	1.26	0.195/20
Z8Y	1530/120	99.54	3.58	0.518/30	1440/1340/10	99.54	1.71	0.276/30

Note: s is standard deviation and n is number of measurements.

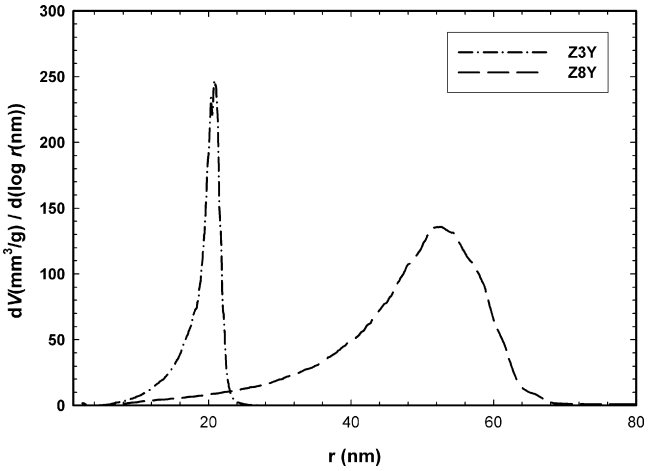

Fig. 6. Pore size distributions of green bodies of zirconia (Z3Y and Z8Y) ceramics.

densities from 98.8% t.d. up to 99.6% t.d. The exact values of the grain size of selected samples are given in Table 3 and the microstructures of the samples can be seen in Figs. 8 and 9.

Mazaeheri et al.[23] found that the grain size of 8 mol% Y_2O_3-doped ZrO_2 decreased by a factor of as much as 7 when using the TSS method instead of the conventional SSS. In contrast to our work they started with zirconia nanoparticles and therefore the temperatures of the second sintering step were very low in their experiments—1050 °C and 950 °C. It is known that the grain growth of 8 mol% Y_2O_3-doped ZrO_2 is suppressed at low temperatures and accelerated at temperatures higher than 1150 °C.[39]

3.4. The influence of crystal structure on the efficiency of Two-Step Sintering of alumina and zirconia ceramics

The above results show that the efficiency of the TSS of oxide ceramics is more dependent on their crystal structure than on their particle size and green body microstructure. In our experiments with alumina and zirconia ceramics the TSS method

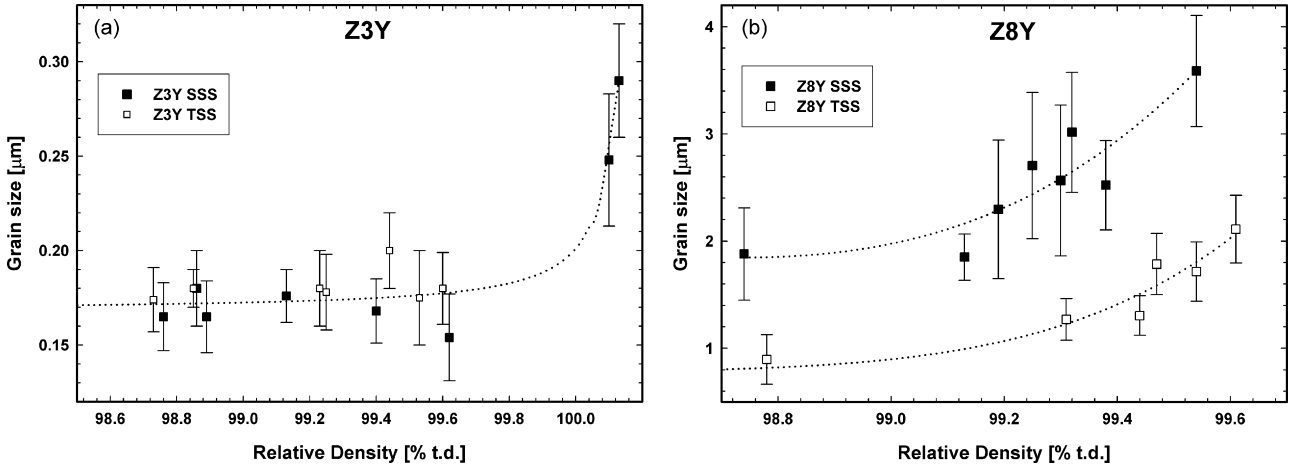

Fig. 7. Dependence of grain size on sintered density of zirconia samples (a, Z3Y and b, Z8Y) sintered by TSS and SSS methods.

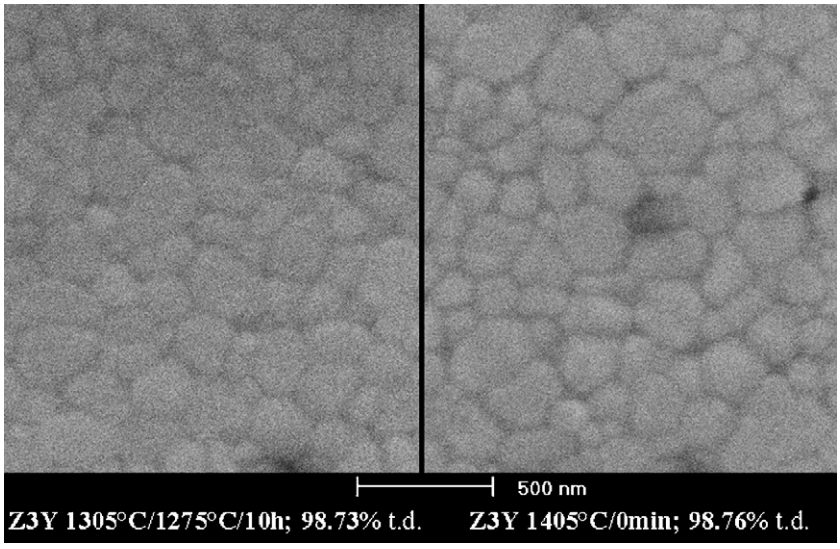

Fig. 8. Microstructure of Z3Y samples sintered to the same density 98.7% t.d. by TSS and SSS cycles.

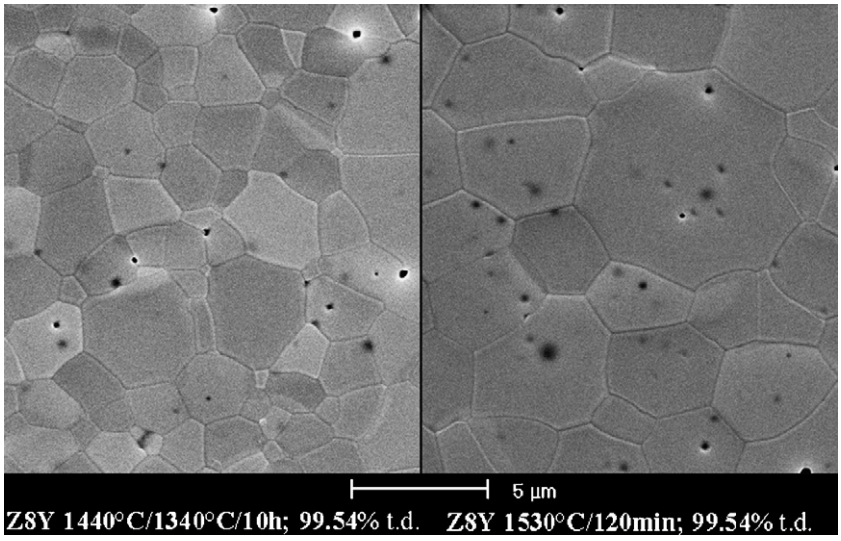

Fig. 9. Microstructure of Z8Y samples sintered to the same density 99.5% t.d. by TSS and SSS cycles.

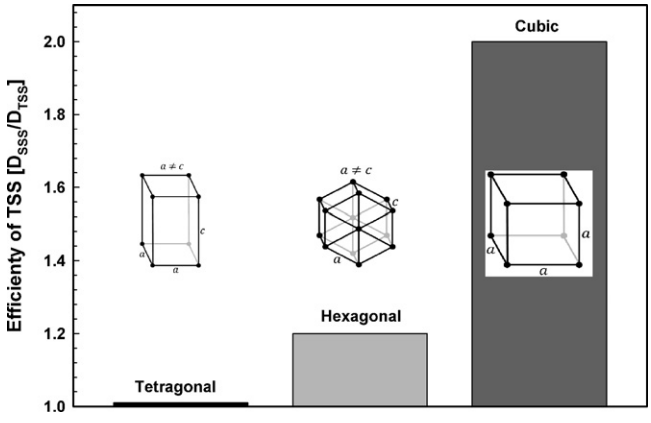

Fig. 10. Ratio of the grain size achieved by SSS to that achieved by TSS for oxide ceramics with different crystal structure.

was applied with great benefit to cubic zirconia ceramics, less success was observed with hexagonal alumina and no effect of TSS method on refining the microstructure of sintered body was recorded in the case of tetragonal zirconia ceramics. Expressing the benefit of the TSS method as a ratio of the grain size achieved by SSS to that achieved by TSS (see Fig. 10), we can see that in our experiments the efficiency of the TSS method increased with increasing ceramic crystal symmetry. At the moment we do not have any evidence to generalize this observation but further experiments with monoclinic, tetragonal and cubic zirconia of the same particle size will be performed to clarify the validity of this hypothesis.

4. Conclusions

The sintering of two types of Al_2O_3 and two types of ZrO_2 (stabilized with 3 mol% Y_2O_3 and 8 mol% Y_2O_3) by the Two-Step Sintering method was studied. The experimental results showed that the efficiency of the Two-Step Sintering of these oxide ceramics was more dependent on their crystal structure than on their particle size and green body microstructure. A remarkable influence of the Two-Step Sintering method on the decrease of grain size of sintered ceramics was observed only for cubic 8 mol% yttria-doped zirconia ceramics (grain size decrease by a factor of 2), for hexagonal alumina this effect was only insignificant (grain size decrease by a factor of 1.2) and for tetragonal 3 mol% yttria-doped zirconia it was not observed at all.

Acknowledgements

The authors gratefully acknowledge the funding provided by the Czech Ministry of Education under grants OC102 (COST 539 Action) and MSM 0021630508. We thank Prof. Z. Shen for valuable discussions, as well as D. Janova for SEM images.

References

1. Dynys, F. W. and Halloran, J. W., Influence of aggregates on sintering. *J. Am. Ceram. Soc.*, 1984, **67**, 596–601.
2. Roosen, A. and Bowen, H. K., Influence of various consolidation techniques on the green microstructure and sintering behaviour of alumina powders. *J. Am. Ceram. Soc.*, 1988, **71**, 970–977.
3. Zheng, J. M. and Reed, J. S., Effects of particle packing characteristics on solid-state sintering. *J. Am. Ceram. Soc.*, 1989, **72**, 810–817.
4. Trunec, M. and Maca, K., Compaction and pressureless sintering of zirconia nanoparticles. *J. Am. Ceram. Soc.*, 2007, **90**, 2735–2740.
5. Coble, R. L. and Gupta, T. G., *Sintering and Related Phenomena*. Gordon and Breach, New York, 1967, pp. 423–441.
6. Gupta, T. K., Possible correlation between density and grain size during sintering. *J. Am. Ceram. Soc.*, 1972, **55**, 276–277.
7. Su, H. H. and Johnson, D. L., Master sintering curve: a practical approach to sintering. *J. Am. Ceram. Soc.*, 1996, **79**, 3211–3217.
8. Wang, J. D. and Raj, R., Estimate of the activation energies for boundary diffusion from rate-controlled sintering of pure alumina, and alumina doped with zirconia or titania. *J. Am. Ceram. Soc.*, 1990, **73**, 1172–1175.
9. Xie, Z. P., Yang, J. L. and Huang, Y., Densification and grain growth of alumina by microwave processing. *Mater. Lett.*, 1998, **37**, 215–220.
10. Maca, K. and Simonikova, S., Effect of sintering schedule on grain size of oxide ceramics. *J. Mater. Sci.*, 2005, **40**, 5581–5589.
11. Mayo, M. J., Processing of nanocrystalline ceramics from ultrafine particles. *Int. Mater. Rev.*, 1996, **41**, 85–115.

12. Kim, B. C., Lee, J. H., Kim, J. J. and Ikegami, T., Rapid rate sintering of nanocrystalline indium tin oxide ceramics: particle size effect. *Mater. Lett.*, 2002, **52**, 114–119.
13. Palmour, H. and Huckabee, M. L., Process for sintering finely derived particulates and resulting ceramics products. U.S. Patent 3,900,542, 19, August 1975.
14. Huckabee, M. L. and Palmour, H., Rate controlled sintering of fine-grained Al_2O_3. *Am. Ceram. Soc. Bull.*, 1972, **51**, 574–576.
15. Agarwal, G., Speyer, R. F. and Hackenberger, W. S., Microstructural development of ZnO using a rate-controlled sintering dilatometer. *J. Mater. Res.*, 1996, **11**, 671–679.
16. Chen, I. W. and Wang, X. H., Sintering dense nanocrystalline ceramics without final-stage grain growth. *Nature*, 2000, **404**, 168–171.
17. Wang, X. H., Chen, P. L. and Chen, I., Two-step sintering of ceramics with constant grain size, I. Y_2O_3. *J. Am. Ceram. Soc.*, 2006, **8**, 431–437.
18. Polotai, A., Breece, K., Dickey, E. and Randall, C., A novel approach to sintering nanocrystalline barium titanate ceramics. *J. Am. Ceram. Soc.*, 2005, **88**, 3008–3012.
19. Karaki, T., Yan, K. and Adachi, M., Barium titanate piezoelectric ceramics manufactured by two-step sintering. *Jpn. J. Appl. Phys.*, 2007, **46**, 7035–7038.
20. Wang, D. H., Deng, X. Y., Bai, H. L., Zhou, H., Qu, W. G. and Li, L. T., Two-step sintering of ceramics with constant grain size, II: $BaTiO_3$ and Ni–Cu–Zn ferrite. *J. Am. Ceram. Soc.*, 2006, **89**, 438–443.
21. Balaya, P., Ahrens, M., Kienle, L., Maier, J., Rahmati, B., Lee, B. S., Sigle, W., Pashkin, A., Kuntsher, C. and Dressel, M., Synthesis and characterization of nanocrystalline $SrTiO_3$. *J. Am. Ceram. Soc.*, 2006, **89**, 2804–2811.
22. Maca, K., Pouchly, V. and Shen, Z. J., Two-step sintering and spark plasma sintering of Al_2O_3, ZrO_2 and $SrTiO_3$ ceramics. *Integrated Ferroelectrics*, 2008, **99**, 114–124.
23. Mazaheri, M., Valefi, M., Razavi, H. Z. and Sarnezhaad, S. K., Two-step sintering of nanocrystalline $8Y_2O_3$ stabilized ZrO_2 synthesized by glycine nitrate process. *Ceram. Int.*, 2009, **25**, 13–20.
24. Ghosh, A., Suri, A. K., Rao, B. T. and Ramamohan, R. T., Low-temperature sintering and mechanical property evaluation of nanocrystalline 8 mol% yttria fully stabilized zirconia. *J. Am. Ceram. Soc.*, 2007, **7**, 2015–2023.
25. Rafferty, A., Prescott, T. and Brabazon, D., Sintering behaviour of cobalt ferrite ceramic. *Ceram. Int.*, 2008, **34**, 15–21.
26. Binner, J., Annapoorani, K., Paul, A., Santacruz, I. and Validhyanathan, B., Dense nanostructured zirconia by two stage conventional/hybrid microwave sintering. *J. Eur. Ceram. Soc.*, 2008, **28**, 973–977.
27. Binner, J. and Vaidhyanathan, B., Processing of bulk nanostructured ceramics. *J. Eur. Ceram. Soc.*, 2008, **28**, 1329–1339.
28. Yu, P. C., Li, Q. F., Fuh, J. Y. H., Li, T. and Lu, L., Two-stage sintering of nano-sized yttria stabilized zirconia process by powder injection moulding. *J. Mater. Process. Technol.*, 2007, **192–193**, 312–318.
29. Li, J. and Ye, Y., Densification and grain growth of Al_2O_3 nanoceramics during pressureless sintering. *J. Am. Ceram. Soc.*, 2006, **89**, 139–143.
30. Granger, G. B., Guizard, C. and Addad, A., Sintering of an ultra pure α-alumina powder. I. Densification, grain growth and sintering path. *J. Mater. Sci.*, 2007, **42**, 6234–6316.
31. Mikoczyova, M. and Galusek, D., Influence of forming method and sintering process on densification and final microstructure of submicrostructure of submicrometre alumina ceramics. *Proc. Appl. Ceram.*, 2008, **2**, 13–17.
32. Bodisova, K. and Sajgalik, P., Two-stage sintering of alumina with submicrometer grain size. *J. Am. Ceram. Soc.*, 2007, **90**, 330–332.
33. Krell, A. and Blank, P., Grain size dependence of hardness in dense submicrometer alumina. *J. Am. Ceram. Soc.*, 1995, **78**, 1118–1120.
34. Krell, A. and Klaffke, D., Effect of grain size and humidity on fretting wear in fine grained alumina, Al_2O_3/TiC and zirconia. *J. Am. Ceram. Soc.*, 1996, **76**, 1139–1146.
35. Krell, A. and Blank, P., The influence of shaping method on the grain size dependence of strength in dense submicrometer alumina. *J. Eur. Ceram. Soc.*, 1996, **16**, 1189–1200.
36. Trunec, M. and Chlup, Z., Higher fracture toughness of tetragonal zirconia ceramics through nanocrystalline structure. *Scripta Mater.*, 2009, **61**, 56–59.
37. Apetz, R. and van Bruggen, M. P. B., Transparent alumina: a light-scattering model. *J. Am. Ceram. Soc.*, 2003, **86**, 480–486.
38. Maca, K., Pouchly, V. and Boccaccini, A. R., Sintering densification curve—a practical approach for its construction from dilatometric shrinkage data. *Sci. Sinter.*, 2008, **40**, 117–122.
39. Shi, J. L., Ruan, M. L. and Yen, T. S., Crystalline growth in yttria-doped superfine zirconia powders and their compacts: a comparison between Y-TZP and ASZ. *Ceram. Int.*, 1996, **22**, 137–142.